Molecular Cell, Vol. 16, 991–1002, December 22, 2004, Copyright ©2004 by Cell Press

DNA Damage Response Pathway Uses Histone Modification to Assemble a Double-Strand Break-Specific Cohesin Domain

Elçin Ünal,[1,2] Ayelet Arbel-Eden,[3] Ulrike Sattler,[3] Robert Shroff,[4] Michael Lichten,[4] James E. Haber,[3] and Douglas Koshland[1,*]

[1]Howard Hughes Medical Institute
Department of Embryology
The Carnegie Institution of Washington
Baltimore, Maryland 21210
[2]Department of Biology
Johns Hopkins University
Baltimore, Maryland 21218
[3]Department of Biology
Rosenstiel Basic Medical Sciences Research Center
Brandeis University
Waltham, Massachusetts 02454
[4]Laboratory of Biochemistry
National Cancer Institute
National Institutes of Health
Bethesda, Maryland 20892

Summary

The postreplicative repair of double-strand breaks (DSBs) is thought to require sister chromatid cohesion, provided by the cohesin complex along the chromosome arms. A further specialized role for cohesin in DSB repair is suggested by its de novo recruitment to regions of DNA damage in mammals. Here, we show in budding yeast that a single DSB induces the formation of a ~100 kb cohesin domain around the lesion. Our analyses suggest that the primary DNA damage checkpoint kinases Mec1p and Tel1p phosphorylate histone H2AX to generate a large domain, which is permissive for cohesin binding. Cohesin binding to the phospho-H2AX domain is enabled by Mre11p, a component of a critical repair complex, and Scc2p, a component of the cohesin loading machinery that is necessary for sister chromatid cohesion. We also provide evidence that the DSB-induced cohesin domain functions in postreplicative repair.

Introduction

DNA damage, including DSBs, triggers a conserved cellular response that involves slowing of cell cycle progression, transcriptional and posttranslational regulation of repair-related proteins, and the recruitment of these proteins to the sites of damage (reviewed in Bradbury and Jackson [2003] and Rouse and Jackson [2002]). This response has been intensively studied because of its importance in fundamental aspects of cell division and its potential relevance to human disease (reviewed in Digweed et al. [1999]; Michelson and Weinert [2000]; and Rotman and Shiloh [1998]).

The DNA damage response is regulated by numerous kinases. The earliest activated kinases, ATM/Tel1p and ATR/Mec1p, subsequently activate additional ones like CHK1/Chk1p and CHK2/Rad53p (reviewed in Jackson [2002] and Shiloh [2003]). Substrates of these kinases include DNA repair-related proteins such as Mre11p, a subunit of the conserved MRX (Mre11/Rad50/Xrs2) and MRN (MRE11/RAD50/NBS1) complexes in budding yeast and humans, respectively (reviewed in D'Amours and Jackson [2002]). The idea that DNA damage repair may also involve proteins linked to chromosome structure and dynamics is supported by the fact that H2AX, a variant of the core H2A histone, is phosphorylated in chromatin surrounding the site of damage (Rogakou et al., 1998, 1999; Shroff et al., 2004).

A key structural component of chromosomes that is also linked to DNA damage is the cohesin complex. Cohesin is an evolutionarily conserved multisubunit complex that consists of four proteins: Mcd1p (Scc1/Rad21), Scc3p (SA1/SA2), Smc1p, and Smc3p (reviewed in Nasmyth [2002]). During an unperturbed cell cycle, cohesin is loaded onto chromosomes during S phase by Scc2p/Scc4p complex and other factors (Ciosk et al., 2000). This loading results in a large domain of cohesins around the centromere and small (1 kb) domains on the arm. In budding yeast, these small domains are called CARs (cohesin-associated regions) and are spaced at 10–15 kb intervals and generally located in AT-rich intergenic sequences (Blat and Kleckner, 1999; Laloraya et al., 2000; Megee et al., 1999; Tanaka et al., 1999). The loading of cohesin serves to hold sister chromatids together from the time of their replication until metaphase-anaphase transition, thus ensuring the biorientation of sister chromatids on the spindle apparatus and their proper segregation (reviewed in Koshland and Guacci [2000]).

In addition to cohesin's role in chromosome segregation, a role in DNA repair is suggested by observations from yeast and mammals. In budding yeast, sister chromatids are the preferred partners for mitotic DSB repair in diploid cells (Kadyk and Hartwell, 1992). Mutants with hypomorphic alleles of cohesin subunits have decreased viability in response to γ irradiation (Birkenbihl and Subramani, 1992; Heo et al., 1998; Sonoda et al., 2001). Furthermore, inactivation of cohesin in S or M phase leads to a reduced efficiency of postreplicative DSB repair. This defect has been attributed to lack of cohesion (Sjögren and Nasmyth, 2001). Because sister chromatid cohesion is established during S phase, the cohesin loaded along the chromosome arms during S phase is thought to be necessary and sufficient for proper postreplicative repair.

Recent cytological studies in mammalian cells indicate that cohesin is recruited to regions of DNA damage (Kim et al., 2002a). This suggests that efficient DNA repair in mammalian cells may require cohesins at the site of DNA damage. Although the damage-induced cohesin binding is intriguing, many questions remain unanswered. What promotes this binding and how is it regulated in response to damage? Is damage-induced cohesin binding important for DNA repair and, if so, what aspect of repair? Is damage-induced cohesin binding unique to mammalian cells, or is it a part of the con-

*Correspondence: koshland@ciwemb.edu

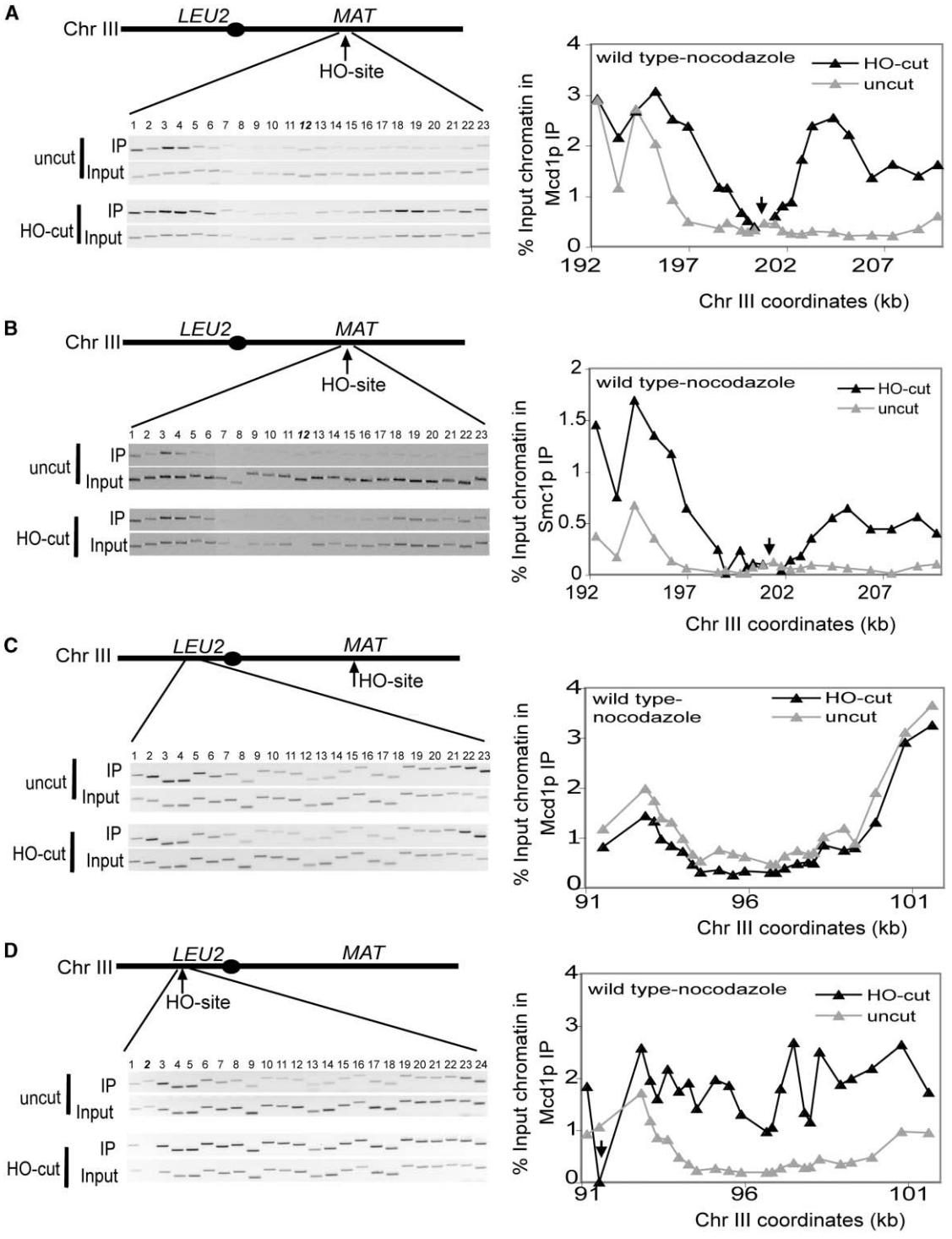

Figure 1. Cohesin Is Enriched around a DSB in M Phase

Cells growing exponentially at 30°C were treated with nocodazole to induce an M phase arrest that was maintained during the entire experiment. After 3 hr 20 min, the culture was split, and galactose was added to one half (HO cut), whereas the other half was grown in the absence of galactose (uncut). After 90 min, cells were fixed with 1% formaldehyde for 2 hr and used for chromatin immunoprecipitation (ChIP, see Experimental Procedures). Input DNA and DNA coimmunoprecipitated with α-HA antibody (IP) were amplified by using primer sets corresponding to sequences around *MAT* or *LEU2*. To ensure the linearity of the PCR signal, appropriate dilutions of IP and input samples were used in PCR amplifications.

(A) The binding of Mcd1p around *MAT* on ChrIII in JKM179-101A (*MCD1HA6*) with (HO cut) or without (uncut) a DSB at *MAT*. Top left, schematic depiction of ChrIII denoting relative positions of *MAT* and *LEU2*. Bottom left, PCR amplified DNA from the left (1–11) and right side (13–23) of HO site were displayed by agarose gel electrophoresis and visualized by ethidium bromide (reverse images are shown). The PCR fragment containing the HO site (*12*) is only present in samples without a DSB. Right, Mcd1p binding profile around *MAT* in samples with (HO cut, black

served DNA damage response common to all eukaryotes?

To address these questions, we examined cohesin binding in response to DSBs in *Saccharomyces cerevisiae*. We show here that a single DSB induces a large domain of cohesin binding near the lesion, demonstrating that the association of cohesin with sites of DSB is an evolutionarily conserved response and likely to be an important part of DNA damage response in all eukaryotes. We also report analyses of this DSB-induced cohesin domain that both define its size, kinetics of assembly, and cell cycle regulation, and that identify evolutionarily conserved factors necessary for its formation. Finally, we provide evidence for one potential role of the DSB-induced cohesin domain in DNA repair. Based on these studies, we propose a model for the assembly of the DSB-induced cohesin domain that is likely to be of general relevance to postreplicative repair in other eukaryotes.

Results

Cohesin Is Enriched around a DSB Site

To investigate cohesin localization in response to a DSB, we used the HO endonuclease to create a single DSB in the genome of *Saccharomyces cerevisiae*. This site-specific restriction endonuclease cleaves a 24 bp degenerate sequence present at the *MAT* locus on chromosome III (ChrIII) (Nickoloff et al., 1986). By using an HO gene under the control of a galactose inducible promoter, it was possible to control the timing of HO expression and DSB formation (Haber, 2002; Jensen and Herskowitz, 1984). This allowed us to study potential changes in cohesin binding at the DSB site both at different stages of the cell cycle and after inactivation of potentially relevant gene products. Repair of the DSB by homologous recombination (HR) was prevented by deletion of the *HML* and *HMR* loci (Moore and Haber, 1996). The persistence of the DSB facilitated the detection of potential DSB-induced changes in cohesin binding.

We first wanted to study cohesin association around a DSB in a cell cycle stage with sister chromatids, a time when cohesin is known to function. Therefore, cells were arrested in M phase with nocodazole, and then a DSB was created by HO induction. The cells were engineered to express only Mcd1p-6HA, the Mcd1 protein with six copies of the hemaglutanin A epitope tag. Chromatin binding of this cohesin subunit was assayed by chromatin immunoprecipitation (ChIP). DNA sequences were amplified from the input chromatin and chromatin immunoprecipitated by anti-HA antibody with 23 primer pairs on either side of the DSB site. For each primer pair, we determined the relative Mcd1p binding by calculating the ratio of the amounts of PCR products in chromatin bound and input samples. The amplified product of each primer pair was also assigned a chromosomal coordinate based upon its sequence alignment with the *Saccharomyces* Genome Database (SGD). Determination of the relative Mcd1p binding for a given chromosomal coordinate allowed us to assess Mcd1p localization at specific chromosome locations in the absence or presence of a DSB.

In the absence of a DSB at *MAT*, there is low Mcd1p binding in a 20 kb region surrounding *MAT*, except for two CAR sites to the left of HO site (Figure 1A, uncut). After 90 min of HO induction, >95% of the DNA is cut (data not shown). At this time, Mcd1p binding around the DSB site has two distinct features. Immediately adjacent to the DSB site is a 2 kb region of low binding that is flanked on either side by 8 kb regions of high binding (Figure 1A). In the 8 kb flanking regions, the maximum DSB-induced increase in Mcd1p binding is approximately 10-fold, with an average of 7-fold for regions that do not contain a CAR site. Thus the presence of a DSB induces a dramatic increase in Mcd1p binding in a domain at least 16 kb in size.

The low Mcd1p binding in the 2 kb region immediately proximal to the DSB partly correlates with a 2-fold reduction in the amplification of input DNA in this region compared to the 8 kb flanking regions. This reduction is not observed in cells without a DSB. Loss of DNA proximal to a DSB at *MAT* has been shown previously, resulting from a 5′–3′ resection activity (Frank-Vaillant and Marcand, 2002; Lee et al., 1998). Thus, nonduplex DNA structure and/or the presence of other break-associated proteins could account for the low Mcd1p binding in the 2 kb region proximal to this DSB.

Having established that a domain of Mcd1p binding is induced in a region surrounding the DSB at *MAT*, we asked three questions about the generality of this observation: (1) whether this induction is specific to this cohesin subunit or the cohesin complex, (2) whether the domain is limited to the DSB region, and (3) whether domains are induced around DSBs at other regions of the genome. To investigate whether the DSB-associated increase in Mcd1p binding reflected an increase in binding of the whole cohesin complex, we used ChIP to monitor the chromatin binding of another subunit of cohesin, Smc1p. To facilitate ChIP, cells were engineered to express only Smc1p-6HA, the Smc1 protein with six copies of the hemaglutanin A epitope tag. Smc1p association at *MAT* locus in cells with and without a DSB show very similar characteristics to Mcd1p association (Figure 1B), with both low binding in the 2 kb region immediately proximal to the break and high levels in the 8 kb flanking regions. We therefore conclude that during M phase, the cohesin complex is enriched around *MAT* locus in response to a DSB. Furthermore, because these strains cannot repair the DSB by HR, there is no repair-associated DNA synthesis. Therefore, the cohesin

bar) and without (uncut, gray bar) a DSB. Percentage of input chromatin in Mcd1p IP is plotted on the y axis versus ChrIII coordinates (kb) on the x axis. Arrow indicates the position of the DSB.

(B) The binding of Smc1p around *MAT* on ChrIII in EU1239 (*SMC1HA6*) with and without a DSB at *MAT*.

(C) The binding of Mcd1p around *LEU2* on ChrIII in JKM179-101A (*MCD1HA6*) with and without a DSB at *MAT*.

(D) Mcd1p binding around *LEU2* on ChrIII. YFP17-101A (*leu2::HO cut-site*, *MCD1HA6*) and YMV150-101A (*leu2, MCD1HA6*) were treated with 2% galactose for HO induction. A DSB at *leu2* was created in YFP17-101A containing the HO site, but not in YMV150-101A.

enrichment around the DSB is independent of DNA synthesis.

To address whether the increased levels of cohesin binding around the DSB at *MAT* was unique to this region, we asked whether a DSB at *MAT* caused an increase in cohesin binding at sites on ChrIII very distal to the DSB or even on other chromosomes. We examined Mcd1p binding around *LEU2*, which is ~110 kb away from *MAT* on the left arm of ChrIII, on the opposite side of the centromere. We detected no significant difference in cohesin binding in this region between cells with and without DSB at *MAT* (Figure 1C). Similarly, no increase in cohesin binding was observed in a region of ChrXII (data not shown). Therefore, the elevated cohesin binding around the DSB at *MAT* is a local response.

This local response is not unique to a DSB at *MAT*. We examined a strain in which the HO recognition site from *MAT* was deleted and moved to *LEU2* (Paques et al., 1998), the region that fails to show increase in cohesin binding when the DSB is at *MAT*. In this region, cohesin binding was monitored on the right side of the DSB, because the left of HO site corresponds to ~7 kb region of repetitive DNA within the Ty element. When the DSB is generated at *LEU2*, cohesin association around the DSB increased in a manner very similar to that observed at *MAT* (Figure 1D), with the exception that cohesin binding was elevated at the *LEU2* DSB even in the 2 kb region immediate proximal to the DSB. This result shows that cohesins can bind near the ends of linear DNA molecules. Furthermore, these results from the *MAT* and *LEU2* loci suggest that a DSB anywhere in the genome induces the formation of a local domain of cohesin.

Cohesin Enrichment around the DSB Is Cell Cycle Regulated and Requires the Scc2p/Scc4p Complex

Given that the expression and function of the cohesin complex is cell cycle regulated (Guacci et al., 1997; Michaelis et al., 1997; Uhlmann and Nasmyth, 1998), we next asked whether cohesin binding at a DSB is also cell cycle regulated. To address this question, we arrested cells at stages of the cell cycle other than M, induced a DSB, and then examined cohesin binding.

In cells arrested in S phase by hydroxyurea treatment, cohesin binding shows increase in the region of a DSB at *MAT* (Figure 2A) and *LEU2* (data not shown), similar to the DSB-specific cohesin loading seen at these loci in M phase. In contrast, no enrichment of cohesin is observed surrounding the DSB site in G1-arrested cells (data not shown). Thus, DSB-specific cohesin localization is cell cycle regulated and occurs in S and M, but not in G1, phase. This is consistent with the absence of the cohesin subunit Mcd1p in G1 phase.

The loading of cohesin on chromosomes at centromeres and CAR sites during S phase requires the activity of Scc2p/Scc4p complex (Ciosk et al., 2000). We asked whether Scc2p/Scc4p is also required for the DSB-specific loading of cohesin. To address this question, strains carrying the *scc2-4* temperature-sensitive allele were arrested at permissive temperature during M phase, allowing the loading of cohesin at centromeres and CAR sites during the preceding S phase. Indeed, the analysis of cohesin binding at the CARC1 and CARC2 region is similar for the *scc2-4* and wild-type (wt) cells, confirming that S phase cohesin loading is not impaired (Supplemental Figure S1 available online at http://www.molecule.org/cgi/content/full/16/6/991/DC1/). Cells were shifted to the restrictive temperature for 1 hr, and HO was induced. The kinetics of DSB formation under these conditions were similar in wt and *scc2-4* cells (data not shown). After 90 min of HO induction, we observed no substantial increase of cohesin levels around the DSB site in *scc2-4* cells at the restrictive temperature (Figure 2B). Therefore, Scc2p is needed for DSB-specific cohesin recruitment as well as for cohesin deposition during S phase. Furthermore, the Scc2p requirement indicates that the cohesin domain at the DSB results from de novo loading rather than the reorganization of already bound cohesin by sliding.

The Assembly of a 100 Kb Cohesin Domain Lags after DSB Formation but Occurs Prior to Completion of DSB Repair

To better characterize the DSB-induced cohesin domain, we asked two additional questions: how large is the domain and how quickly does it form? To investigate the kinetics of cohesin enrichment around the DSB site, M phase-arrested cells were collected at different time points after HO induction. The amount of HO-cut DNA was determined by Southern blotting and the levels of cohesin were compared by ChIP against Mcd1p subunit.

After 10 min of HO induction, ~50% of the cells contain a DSB (Figure 3A, left). At this time point, there is no detectable increase in cohesin binding around the DSB site. Increased cohesin binding is apparent 45 min after HO induction and intensifies at 90 min (Figure 3A, right). This result shows that there is a lag period for cohesin loading after the formation of a DSB, suggesting that cohesin loading may require a prior activation of another DSB-induced event. In addition, in strains capable of repair by HR, DSB-induced cohesin enrichment and HR occur in a similar time frame (data not shown). Thus, cohesin enrichment around the DSB occurs within a period required for repair by HR.

Our initial studies on DSB induced cohesin domain examined a region limited to 10 kb on both sides of the DSB at *MAT* locus. To see how far away from the DSB site cohesin enrichment spreads, we looked at Mcd1p levels in M phase-arrested cells around the *MAT* locus. Cohesin binding in this region is low, making the extended analysis of DSB-induced cohesin binding easier (Blat and Kleckner, 1999; Glynn et al., 2004).

90 min after HO induction, the DSB-induced cohesin domain extends ~40 kb to the left and ~50 kb to the right of the DSB (Figure 3B, top). More than half of the sites assayed within the domain have at least a 5-fold increase in Mcd1p binding after induction of the DSB (Figure 3B, bottom); sites with no increase in Mcd1p binding correspond to preexisting cohesin sites or sequences immediately adjacent to the DSB (Figure 3B). Sites with a greater than 5-fold increase are distributed throughout the domain in regions of high GC content and in both intra and intergenic regions (data not shown). This data show that in response to a single DSB, cohesins bind apparently irrespective of sequence over a large domain around this lesion, about one-third of the size of ChrIII.

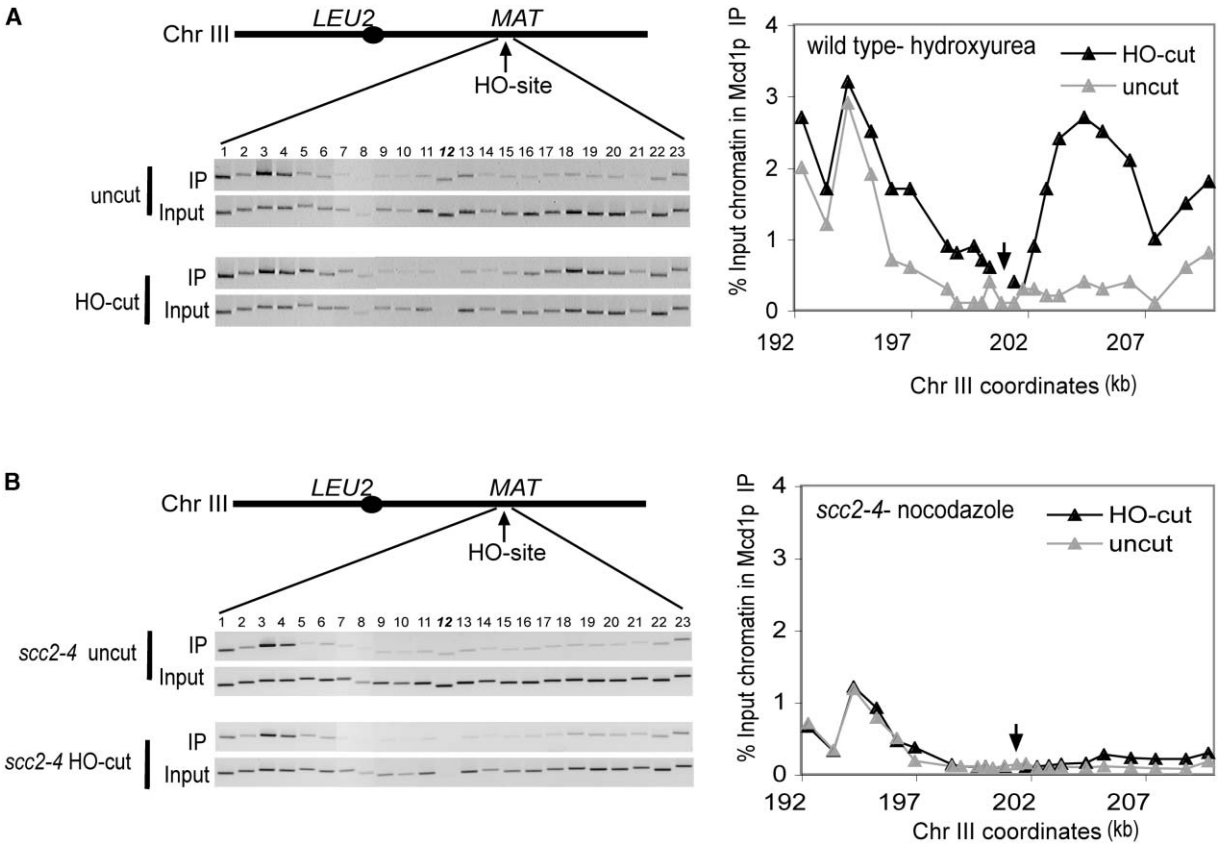

Figure 2. Cohesin Enrichment around the DSB Occurs in S Phase and Is Dependent on Scc2p/Scc4p

(A) Mcd1p binding around *MAT* on ChrIII during S phase in JKM179-101A (*MCD1HA6*) with and without a DSB at *MAT*. Samples for ChIP were prepared as described in Figure 1, except cells were treated with hydroxyurea to induce an arrest in S.

(B) The binding of Mcd1p around *MAT* on ChrIII in EU1234 (*MCD1HA6*, *scc2-4*) with and without a DSB at *MAT*. Cells growing exponentially at 23°C were treated with nocodazole. After 5 hr, temperature was shifted to 30°C for 1 hr to inactivate scc2p. HO induction and ChIP-PCR analysis were done as described in Figure1.

Cohesin Enrichment around the DSB Is Regulated by the DNA Damage Checkpoint and Requires H2AX Phosphorylation

The formation of a large cohesin domain surrounding a DSB site suggested that the DNA damage response pathway might be required for cohesin recruitment to the DSB site. To test this possibility, we examined the dependency of cohesin binding around the DSB site on Mec1p and Tel1p, two key kinases needed for DSB checkpoint response. Wt, *mec1*Δ, *tel1*Δ, or *mec1*Δ *tel1*Δ double mutant cells were arrested in M phase, a DSB at *MAT* was generated by HO induction, and cohesin binding was determined by ChIP against Mcd1p. The results indicate that Mec1p or Tel1p kinase alone can promote cohesin enrichment around the DSB site (Figure 4A), although to a lesser extent when compared to wt. Mec1p appears slightly more important than Tel1p, because the levels of cohesin around the DSB are lower in *mec1*Δ cells than in *tel1*Δ (Figures 4A and 4B). In contrast, in the *mec1*Δ *tel1*Δ double mutant, there is very little cohesin enrichment surrounding the DNA lesion (Figures 4A and 4B). Thus, Mec1p and Tel1p kinases act redundantly to promote the formation of the DSB-specific cohesin domain.

The redundant requirement for Mec1p and Tel1p suggested that they might phosphorylate a common downstream target necessary for cohesin enrichment around the DSB site. One attractive candidate was histone H2AX. Histone H2AX comprises the major histone H2A pool in yeast (from here on referred to as H2AX) and is phosphorylated in the vicinity of a DSB by the activity of Mec1p and Tel1p (Downs et al., 2000; Redon et al., 2003).

To address a possible role for phosphorylated H2AX (γ-H2AX) in the DSB-induced cohesin domain, we examined the pattern of γ-H2AX around *MAT*-DSB site in M phase-arrested cells by ChIP with a γ-H2AX specific antibody. No detectable γ-H2AX is observed in the absence of a DSB around *MAT* locus. After 90 min of HO induction, γ-H2AX levels increase 60 kb on both sides of the DSB (Figure 4C). Levels of γ-H2AX, like cohesin, are also low in the region immediately adjacent to the DSB (Figure 4C and Shroff et al., 2004). The boundaries of the DSB-induced cohesin domain lie within the induced domain of γ-H2AX. Therefore, this DSB-specific chromatin modification might be a signal for cohesin enrichment. In order to test this possibility, we examined DSB-induced M phase cohesin binding around *MAT* in *hta1-S129A hta2-S129A* strains, where the damage-induced H2AX phosphorylation is blocked (Downs et al., 2000). In *S129A* mutants, there is no increase of Mcd1p

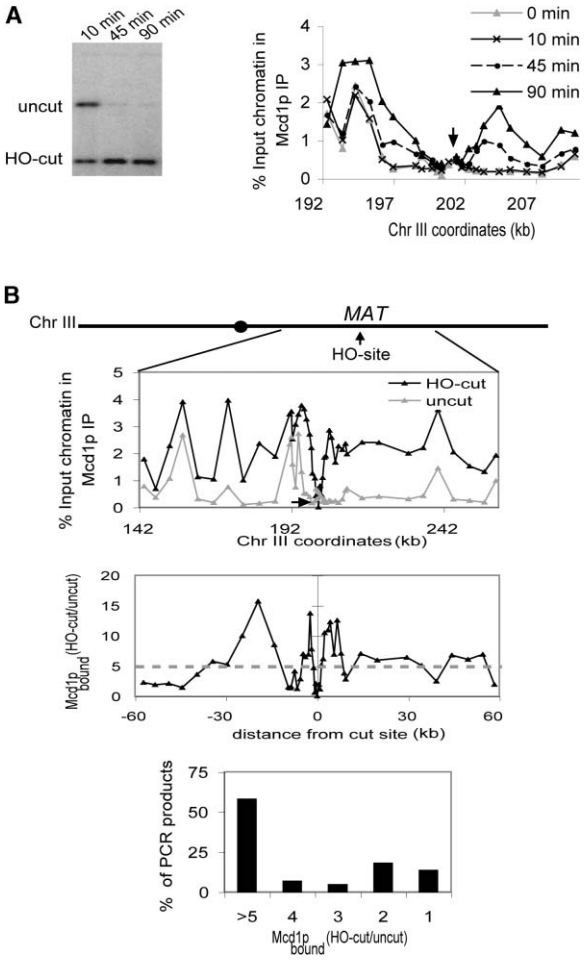

Figure 3. Cohesin Binding around the DSB Is Detected 45 Min after HO Induction and Extends to a ~100 Kb Region Surrounding the DSB

(A) Kinetics of cohesin binding around *MAT* in JKM179-101A (*MCD1HA6*) after DSB formation. Cells growing exponentially at 30°C were treated with nocodazole to induce an M phase arrest that was maintained throughout the experiment. Aliquots of cells taken at indicated time points were analyzed for HO-cutting efficiency (left, Southern blot) and for Mcd1p binding by ChIP PCR (right).

(B) Extended analysis of cohesin binding around *MAT* DSB site in M phase. Top, Mcd1p binding profile on a 120 kb region around *MAT* in JKM179-101A (*MCD1HA6*) with and without a DSB. Middle, increase in Mcd1p binding after DSB formation (y axis, see text for details) is plotted as a function of distance (x axis) from the DSB-site (x = 0). $Mcd1_{bound}$ (HO cut/uncut) is calculated by dividing the percentage of input chromatin in Mcd1 IP of HO cut samples by the percentage of input chromatin in Mcd1p IP of uncut samples. Bottom, the percentage of PCR products is plotted on the y axis versus $Mcd1p_{bound}$ (cut/uncut) on the x axis.

around the DSB site, suggesting that H2AX S129 phosphorylation is required for the assembly of the large cohesin domain surrounding the DSB (Figure 4D).

Rad53p and Mre11p Promote Cohesin Enrichment around the DSB, and Mre11p Acts Independently from γ-H2AX

Rad53p and Mre11p are two other proteins that are important for DNA damage and have been linked to cohesin. Rad53p is a kinase that modifies a number of proteins in response to DNA damage, including the Mcd1p subunit of cohesin (Sidorova and Breeden, 2003). In MRE11-mutated human ATLD2 cells, cohesin fails to cluster at laser-induced damage (Kim et al., 2002a). We asked if Mre11p or Rad53p act in DSB-induced cohesin recruitment in yeast by examining cohesin levels around the *MAT*-DSB in M phase arrested *mre11*Δ or *rad53*Δ cells. After 90 min of HO induction, no significant cohesin domain is observed in the *mre11*Δ mutant (Figure 5B), and the domain is partially reduced in the *rad53*Δ mutant (Figure 5A). In contrast, a mutation in the DNA repair factor ligase 4 had no effect on DSB-induced cohesin recruitment (data not shown). These results suggest that early, but not late, components of the DNA damage pathway are essential for stable assembly of the DSB-induced cohesin domain.

It has been recently shown that the MRE11/RAD50/NBS1 complex increases the in vitro activity of ATM kinase (Lee and Paull, 2004). Therefore, we asked if γ-H2AX around the DSB region is altered in *mre11*Δ cells. The size of the DSB-induced γ-H2AX region does not change in *mre11*Δ mutants, and the level of γ-H2AX around the DSB is only slightly reduced in this mutant compared to wt (Figure 5C). From this, we conclude that Mre11p is dispensable for γ-H2AX formation in M phase-arrested cells. Thus, an Mre11p function independent of γ-H2AX formation is required for the assembly of the large DSB-induced cohesin domain.

Cohesin Is Important for Efficient Postreplicative Repair, but Not for Regulating Intrachromosomal Gene Conversion or for Single-Stranded DNA Formation at the DSB Ends

Because a DSB-induced cohesin domain forms in S and M phases, but not G1, it seemed likely that this domain might be important for replicative/postreplicative repair using sister chromatids. Because HO endonuclease generates breaks in both sister chromatids, it cannot be used to assess sister chromatid-based repair. Therefore, we used γ irradiation to generate DSBs in wt and *scc2-4* cells that were arrested in M phase at 23°C. Cells were shifted to 30°C prior to irradiation to inactivate scc2-4p function and thus to prevent DSB-specific cohesin loading. The relative survival after irradiation was 3-fold lower in *scc2-4* cells than in wt cells (data not shown), suggesting that the DSB-induced cohesin domain is important for DSB repair. To test whether this decrease in viability reflected an inability to repair DSBs specifically during M phase, we assayed chromosome breakage and repair in wt and *scc2-4* cells on pulsed-field gels. For both wt and *scc2-4* cells, the fraction of ChrXV that was broken by irradiation was 31% and 43% for 320 and 160 Gy, respectively (Figure 6A and data not shown). Of the broken chromosomes, the fraction that was repaired to full length at either dose was ~3-fold greater in wt than in *scc2-4* (Figure 6B). *H2AX S129A* mutants, which are also compromised for DSB-induced cohesin loading, exhibit a similar decrease in viability and DSB repair (data not shown). Thus, the formation of DSB-induced cohesin domain is important for post-replicative repair.

Postreplicative DSB repair is likely to occur by recom-

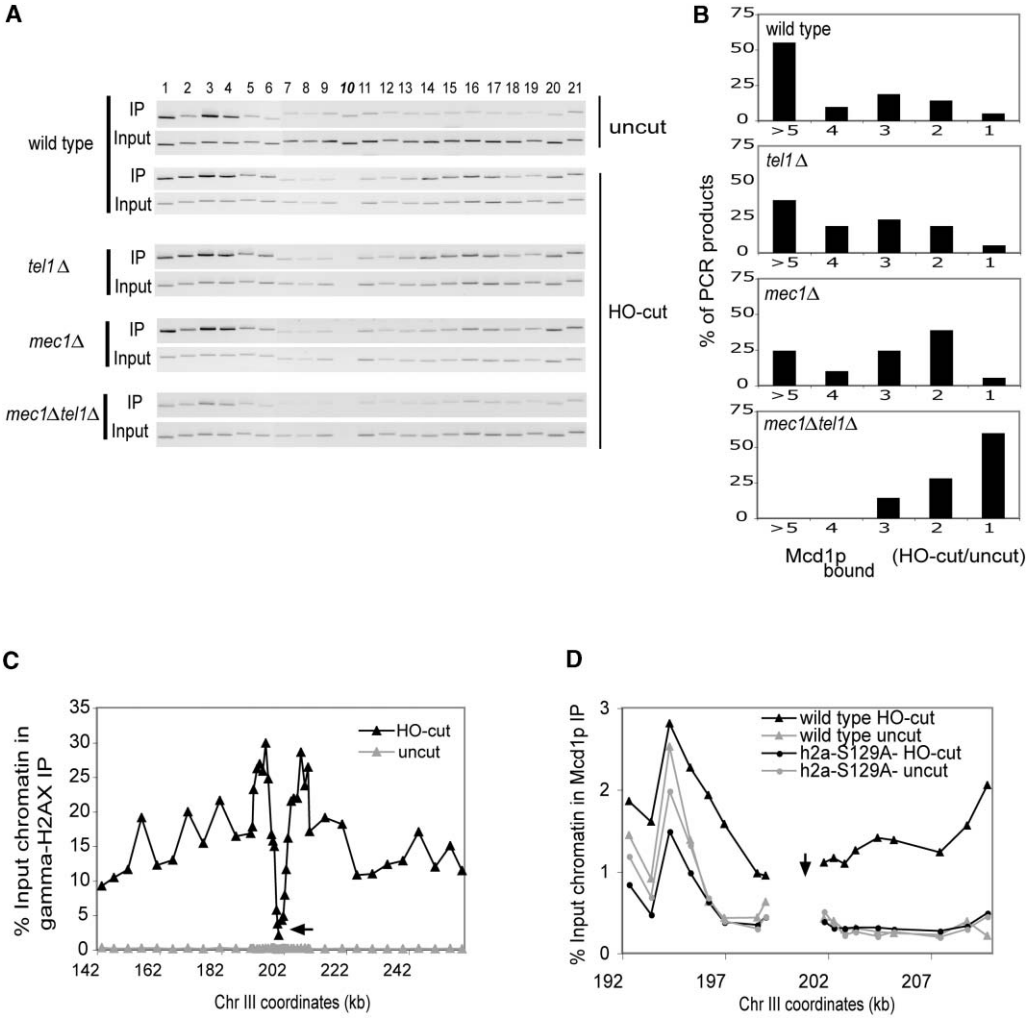

Figure 4. Cohesin Binding around the DSB Is Dependent on Mec1p or Tel1p and the Phosphorylation of Their Common Downstream Target, H2AX

Analysis of cohesin binding around the *MAT* DSB site in JKM179-101A (*MCD1HA6*), EU1242 (*MCD1HA6*, *tel1::NAT*), EU1244 (*JKM179-101A*, *mec1::NAT, sml1::KANMX*) and YAA47-101A (*MCD1HA6*, *mec1::NAT, tel1::TRP1, sml1::KANMX*). Samples for ChIP were prepared as described in Figure 1.

(A) PCR-amplified DNA from the left (1–9) and right side (11–21) of HO site. The PCR fragment *10* is amplified from the sequence containing the HO site.

(B) Comparison of the increase in cohesin binding around the *MAT* DSB site in wt, *tel1*Δ, *mec1*Δ, and *mec1*Δ *tel1*Δ cells. $Mcd1p_{bound}$ (HO cut/uncut) is quantified with PCR products from 44 primer sets corresponding to sequences around the *MAT* DSB site. The percentage of PCR products is plotted on the y axis versus $Mcd1p_{bound}$ (cut/uncut) on the x axis (see Figure 3).

(C) Distribution of γ-H2AX around the *MAT* DSB site in JKM179-101A with and without a DSB.

(D) Analysis of cohesin binding around the *MAT* DSB site in YUS020-101A (*MCD1HA6*) and YUS022-101A (*MCD1HA6, hta1S129A, hta2S129A*). Relative Mcd1p binding is not included for five primer sets amplifying sequences from SGD199535→SGD201576 because these primer sets also yield products from *HML* and *HMR* loci.

bination between sister chromatids. The defect in postreplicative repair in the absence of DSB-specific cohesin domain could be due to a defect that specifically affects sister chromatid recombination or a general defect in HR. To test the role of DSB-induced cohesin domain in general HR, we examined two different HO-induced intrachromosomal gene conversion events, between *MAT* and *HML* and between *LEU2* (*leu2*^{HO}) and a second copy of *LEU2* (*leu2*$^{R-}$) integrated at *HIS4*. In both instances, similar levels of gene conversion occurred in wt and cohesin mutants (Figures 7A and 7B), suggesting that cohesin is not required for intrachromosomal gene conversion. In addition, cohesin does not seem to prevent HR, because the *leu2*$^{R-}$ donor sequence at *HIS4* lies within the cohesin domain induced by the DSB at *leu2*^{HO} (data not shown).

A second aspect of HR is 5′–3′ resection of DSB ends. To test whether resection rate is regulated by the DSB-specific cohesin domain, we examined the resection of the DSB at *MAT* in wt, *mre11*Δ, and *scc2-4* cells. Cells were arrested in M phase at 23°C and were then shifted to 30°C to inactivate DSB-specific cohesin binding in the *scc2-4* strain. HO was induced to create a DSB, and samples were collected at different time points to

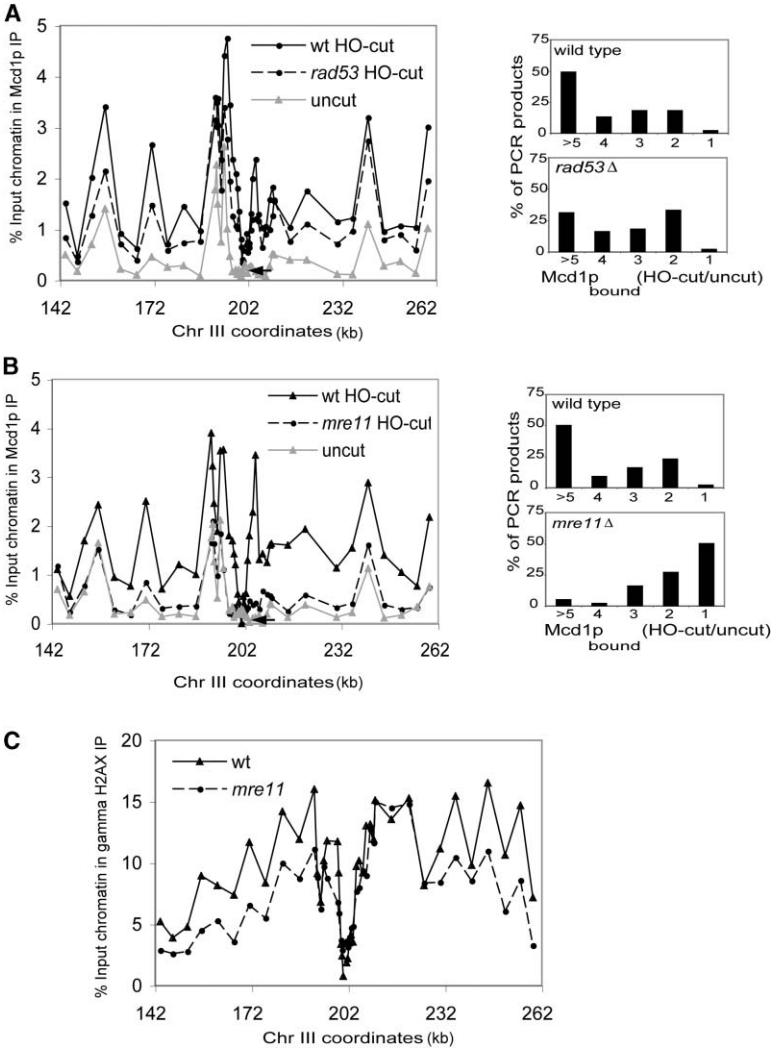

Figure 5. Mre11p and Rad53p Are Required for the Formation of the DSB-Specific Cohesin Domain, but Not the γ-H2AX Domain

Analyses of cohesin binding and γ-H2AX around the *MAT* DSB site in *rad53*Δ and *mre11*Δ mutants. Samples for ChIP were prepared as described in Figure1.

(A) Distribution and fold increase in cohesin binding around *MAT* in JKM179-101A (*MCD1HA6*) and EU1231 (*MCD1HA6*, *rad53::NAT, sml1::KANMX*) with and without a DSB.

(B) Distribution and fold increase in cohesin binding around *MAT* locus in JKM179-101A (*MCD1HA6*) and EU1204 (*MCD1HA6*, *mre11::KANMX*) with and without a DSB.

(C) Distribution of γ-H2AX around the DSB at *MAT* in wt (JKM179-101A) and *mre11*Δ (EU1204) cells.

monitor resection. In agreement with the previous reports (Ivanov et al., 1994; Lee et al., 1998), *mre11*Δ cells slow the resection rate relative to wt, whereas *scc2-4* cells have a similar rate as wt (Figure 7C). Thus, the DSB-specific cohesin domain does not affect 5′–3′ resection rate. Taken together, these results suggest that DSB-induced cohesin domain is required for a process specific to sister chromatid repair.

Discussion

In budding yeast, cohesin is recruited to chromosomes specifically in response to DSBs (Ström et al., 2004 [this issue of *Molecular Cell*]). Similarly, in mammalian cells chromosomal binding of cohesins is stimulated by DNA damage (Kim et al., 2002a). In both yeast and mammalian cells, the damage-induced cohesin binding is restricted to regions of damage and occurs within a physiological time frame (Kim et al., 2002a; this study). The fact that the induction of cohesin binding upon DNA damage occurs in divergent species and with similar properties suggests that it is likely an important cellular response to chromosome damage in all eukaryotes. This importance is underscored further by the fact that cohesin binding is induced by a single DSB (Ström et al., 2004).

The assembly of the large cohesin domain flanking the DSB is controlled by the DNA damage checkpoint pathway through the Mec1p/Tel1p kinases (this study). These kinases and their mammalian orthologs, ATR and ATM, are the master regulators of the DNA damage response (reviewed in Shiloh [2001]). Our study shows that one way these kinases regulate cohesin binding in budding yeast is by phosphorylating H2AX. Both in budding yeast and mammals, H2AX phosphorylation is stimulated by DNA damage and requires the redundant activities of Mec1p/ATR and Tel1p/ATM kinases (Burma et al., 2001; Downs et al., 2000; Redon et al., 2003; Stiff et al., 2004; Ward and Chen, 2001; Shroff et al., 2004). DSB-induced cohesin loading also requires the MRX complex component Mre11p and, to a lesser extent, Rad53p, a CHK2 kinase homolog (this study). MRE11 has also been shown to be required for cohesin recruitment to sites of DNA damage in mammals (Kim et al., 2002a). Because the assembly of the DSB-induced cohesin domain requires conserved components of the DNA damage response, the mechanism for the assem-

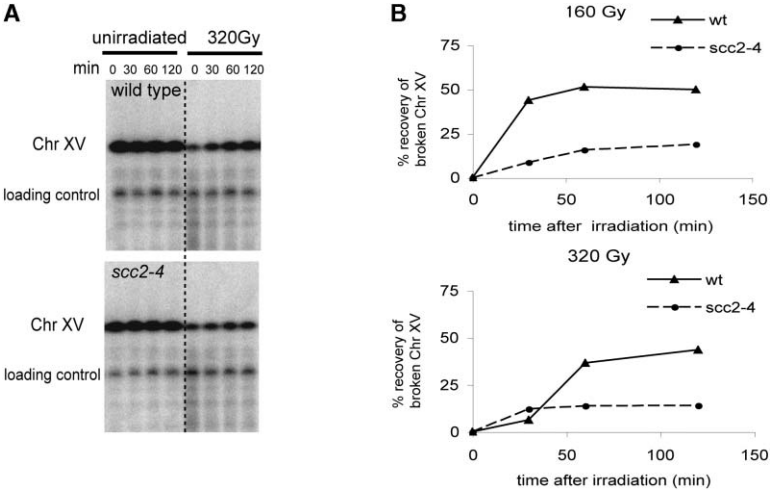

Figure 6. DSB-Specific Cohesin Is Required for Efficient Postreplicative Repair

Cells from JKM179-101A (*MCD1HA6*) and EU1234 (*MCD1HA6*, *scc2-4*) strains growing exponentially at 23°C were treated with nocodazole to induce an M phase arrest that was maintained throughout the experiment. After 3 hr 30 min, temperature was shifted to 30°C to inactivate scc2p. After 1 hr, both wt and *scc2-4* cell cultures were split and one-half of the cultures was irradiated with 320 Gy. Aliquots were taken at 0, 30, 60, and 120 min after irradiation, fixed with 70% ethanol, and processed for pulsed-field gel electrophoresis (PFGE). For the same time points, aliquots were also collected from the unirradiated cultures. For internal loading control, all samples were mixed with a fixed amount of PHY112 cells in which *HIS3* is present on ChrII instead of ChrXV.

(A) After PFGE, yeast chromosomes were transferred to membrane and hybridized with a radioactive probe specific to HIS3 to detect ChrXV from the time-course samples and Chr II from the loading controls. SD of the radioactive signal intensity for the nonirradiated samples is 10%.

(B) Recovery in wt and *scc2-4* cells after 160 Gy and 320 Gy irradiation. ChrXV intensity is normalized to the ChrII intensity for all lanes. The percentage of the repair of the broken ChrXV is plotted on the x axis versus time (min) on the y axis. The percentage of the repair of broken ChrXV is calculated by $(I_x\text{-}I_0)/(1\text{-}\ I_0/I_u)$, by using the intensities of ChrXV prior to irradiation(I_u), immediately after irradiation (I_0), and during the recovery after irradiation (I_x).

bly of this domain (see below) is likely to be conserved between yeast and other eukaryotes.

In this study, we show that the DSB-induced cohesin domain correlates with the size of γ-H2AX domain, and DSB-induced cohesin binding is completely absent in nonphosphorylatable H2AX mutants. These two observations identify γ-H2AX as a target for the damage-induced recruitment of cohesin in the vicinity of DSBs. The recruitment of cohesins by γ-H2AX explains why cohesin binding spreads continuously from the DSB and is not subject to the normal constraints of arm cohesion imposed by transcription and AT content. It also provides a functional explanation for why H2AX is phosphorylated over such a widespread region surrounding breaks in both yeast and mammalian cells (Rogakou et al., 1999; Shroff et al., 2004). A different histone modification, methylation of H3, has also been established as being important for recruitment of cohesins to heterochromatin in *S. pombe* (Bernard et al., 2001; Nonaka et al., 2002; Partridge et al., 2002). Therefore, different histone modifications are used to recruit cohesin to different chromosome targets, just as they recruit transcription machinery to different promoters.

Cohesin enrichment around the DSB region requires two independent events, because H2AX phosphorylation is not required for association of Mre11p with DSBs (Shroff et al., 2004), and Mre11p is dispensable for the formation of the γ-H2AX domain (Shroff et al., 2004; this study). We suggest that in response to a DSB, phosphorylation of H2AX by Mec1p and Tel1p generates a large domain of γ-H2AX, which is permissive for cohesin binding and defines the size of the DSB-specific cohesin domain. Mre11p at the DSB enables cohesin binding, possibly through a direct interaction (Kim et al., 2002a). Mre11p might also promote cohesin binding by supporting the formation of single-stranded DNA (ssDNA), which could activate Rad53p and potentially other kinases. These kinases could in turn stimulate cohesin loading, possibly by phosphorylating cohesin subunits (Kim et al., 2002b; Kitagawa et al., 2004; Sidorova and Breeden, 2003; Yazdi et al., 2002). This putative mechanism is consistent with the lag in Rad53p activation and the lag in assembly of the cohesin domain (Pellicioli et al., 2001; this study). The regulation of cohesin loading by ssDNA is attractive because DSB-induced cohesin binding is likely to be important for recombination between sister chromatids, and ssDNA formation is an early step in the commitment to repair by recombination.

DSB-specific cohesin loading is required for the efficient postreplicative repair of DSBs (Ström et al., 2004). Previous studies suggested that postreplicative DSB repair requires sister chromatid cohesion established by cohesin loading along the chromosome arms during S phase (Sjögren and Nasmyth, 2001). However, because the inactivation of DSB-induced cohesin loading also perturbs postreplicative repair (Ström et al., 2004), we propose that postreplicative repair requires DSB-induced cohesin binding to promote local sister chromatid cohesion. In fact, elegant functional analyses suggest that the DSB-induced cohesin loading can mediate cohesion (Ström et al., 2004). Furthermore, DSB-induced cohesin domains form only in phases of the cell cycle when sister chromatids are present and require Scc2p, a factor known to be required for cohesion (Ström et al., 2004). The requirement for damage-induced cohesion in repair might explain why the cells retain the ability to load cohesins outside of S phase.

The requirement for DSB-induced cohesin for efficient postreplicative repair raises two interesting questions. First, how is cohesion generated outside of S phase, when previous studies had suggested an obligatory step for cohesion establishment in S phase (Uhlmann and Nasmyth, 1998)? This obligatory step could be a specialized structure that occurs during DNA synthesis. Out-

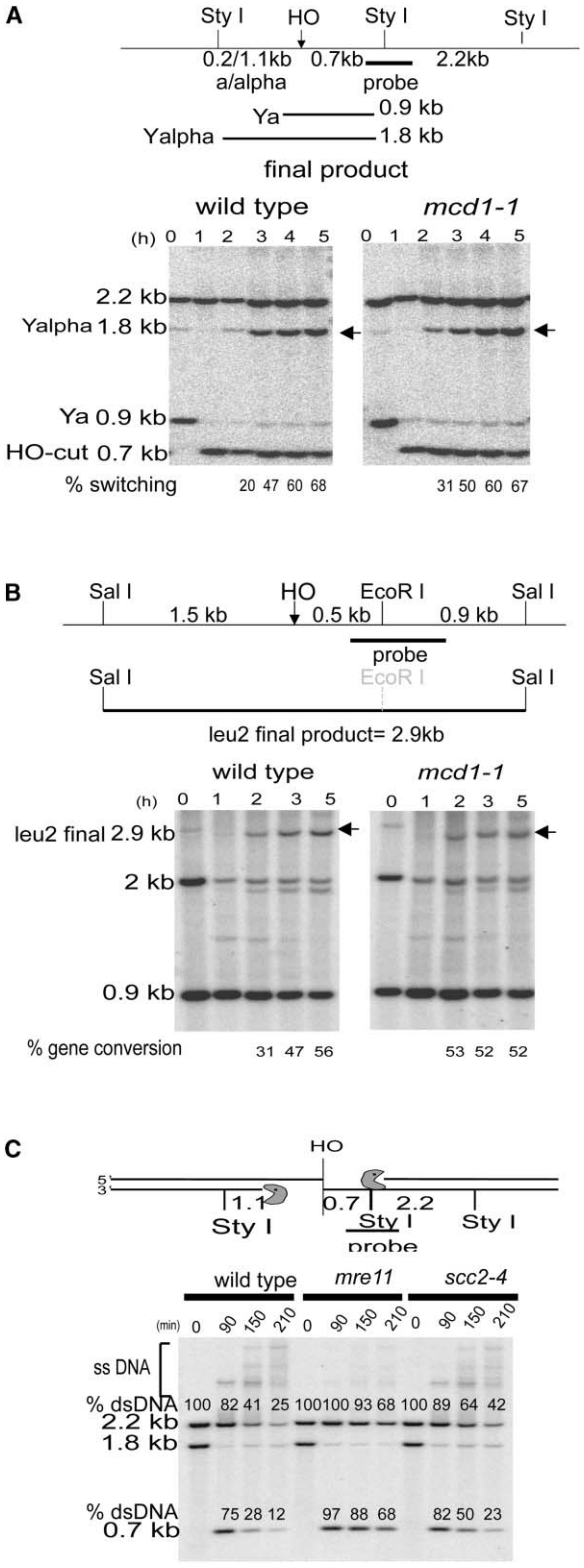

Figure 7. DSB-Specific Cohesin Is Not Required for Intrachromosomal Gene Conversion or 5′–3′ Resection

(A) Mating type switching in JH2004-1A and JH2004-12A. Cells growing exponentially at 23°C were treated with nocodazole to induce an M phase arrest that was maintained throughout the experiment. After 5 hr, temperature was shifted to 34°C and was kept at 34°C during the course of the experiment. After 1 hr at 34°C, galactose was added to the medium (time 0 hr). 1 hr after the addition of galactose, dextrose was added to the medium to repress HO (time 1 hr). Aliquots were taken at indicated time points for genomic DNA preparation (see Experimental Procedures). Top, *Sty I* restriction map of the region containing the *MAT* DSB site (HO). Bottom, Southern blotting was used to monitor the DSB-induced gene conversion event. The probe hybridizes to the *MAT*a specific (Ya, 0.9 kb) sequence prior to HO induction and to the *MAT*α specific (Yα, 1.8 kb) sequence after gene conversion. The arrow points to the *MAT*α specific final product for switching. The quantification of gene conversion of *MAT*a to *MAT*α (% switching) is presented beneath each lane.

(B) Gene conversion at *LEU2* in EU1294 and EU1300. Samples were prepared as described in (A) except the temperature was shifted to 37°C. Top, restriction map of the *LEU2* containing the DSB site (HO). The $leu2^{R-}$ donor sequence (not shown) is integrated at *HIS4* on ChrIII and lacks the HO site as well as the EcoRI and SalI sites on the right side of HO site. Bottom, Southern blotting was used to monitor the DSB-induced gene conversion events. One of the gene conversion products (2.9 kb *LEU2* final, indicated by the black arrows) can be detected after EcoRI-SalI digest by using the probe shown on top. The faster migrating band around 2 kb region corresponds to a gene conversion product that lost the HO site but retained the *EcoR I* site. The quantification of gene conversion of $leu2^{HO}$ to $leu2^{R-}$ (% gene conversion) is presented beneath each lane.

(C) Analysis of 5′–3′ resection in JKM179-101A, EU1204, and EU1234. Samples were prepared as described in (A) except the temperature was shifted to 30°C. StyI digested DNA was run on an agarose gel, transferred to membrane and hybridized with a probe shown in top. The single-stranded DNA (ssDNA) due to 5′–3′ resection becomes resistant to StyI digest and appears as slow migrating heterogeneous bands. The loss of signal intensity in the 0.7 and 2.2 kb StyI restriction digest products also indicates the formation of ssDNA.

side of S, this structure for cohesion establishment could be generated by repair-associated DNA synthesis although the loading of cohesin at DSBs can occur in the absence of repair-associated DNA synthesis (this study). Alternatively, the establishment of cohesion may simply require the close proximity of sister chromatids. In S phase, this proximity is achieved immediately behind the replication fork. For DSB-induced cohesion in M phase, this proximity could be achieved by the cohesion generated along the arms during S phase or possibly by the MRX complex. If proximity is sufficient for cohesion, this will greatly simplify the in vitro reconstitution of cohesion.

The second question raised by DSB-induced sister chromatid cohesion is how does it promote postreplicative repair between sister chromatids? DSB-induced cohesion is unlikely to affect general aspects of recombination, as inactivation of cohesin neither perturbs gene conversion between dispersed sequences nor resection (this study). Tethering the broken DNA ends close to the sister chromatid may make it the preferred substrate for repair, preventing the highly-reactive ends from undergoing aberrant reactions that lead to translocations, large interstitial deletions, and loss of heterozygosity. Therefore, DSB-induced cohesin loading may play an important role in the maintenance of genomic integrity.

Experimental Procedures

Yeast Strains and Plasmids

Information about yeast strains and plasmids is available online in the Supplemental Data.

Cell Synchronization

Exponentially dividing cell cultures were grown in YEP media (Guthrie and Fink, 1991) with 3% glycerol (EMD, 30% v/v stock) and 2% lactic acid (Fisher, 40% v/v stock [pH 5.7]) and then arrested in G1, S, or M phase by the addition of 3×10^{-6} M α-factor (Sigma), 130 mM hydroxyurea (HU) (Sigma), or 15 μg/ml nocodazole (Sigma), respectively. Cells used for irradiation experiments were grown in YEP media supplemented with 2% dextrose (EM Science, 20% w/v stock).

Culture Conditions for HO Induction

For HO induction, cells were grown to approximately 0.6×10^7 cells/ml. In strains with a stably integrated *GAL10::HO* sequence, cells were grown in YEP media with 3% glycerol and 2% lactic acid. In strains carrying the *GAL10::HO* sequence on a centromeric plasmid, selective synthetic medium supplemented with 3% glycerol and 2% lactic acid was used to retain the plasmid. Cells were then arrested as described above, and subsequently D-galactose (Sigma, 20%w/v stock) was added to the culture at a final concentration of 2% w/v. For analysis of gene conversion, in order to repress *HO*, dextrose was added to the culture at a final concentration of 2% w/v, 1 hr after D-galactose addition.

ChIP

ChIP was performed as described (Megee et al., 1999). Immunoprecipitations (IPs) were done with 12CA5 anti-HA antibody (Roche) or rabbit polyclonal antiserum against the yeast-specific H2AX phosphopeptide (kindly provided by Christophe Redon, NCI, NIH). Input DNA was diluted 100-fold (HA IP) or 6.25-fold (γ-H2AX IP) relative to immunoprecipitated DNA before PCR analysis.

PCR and Data Analysis

Information about the primers used in this study is available upon request. A 50 μl PCR reaction contained 3 μl template DNA, 50 mM KCl, 10 mM Tris-HCl ([pH 9.0] at 25°C), 0.1% Triton X-100, 1.5 mM $MgCl_2$, 0.2 mM of each dNTP, 50 pmole of each oligonucleotide, and 2.5 units of Taq polymerase (Promega). PCR reactions were 26 cycles of 95°C, 30 s; 57°C, 45 s; and 72°C, 60 s done with a PTC-200 Peltier thermal cycler from MJ research. PCR products were resolved on 2.5% agarose gels (NuSieve) in 1$\times$ TBE buffer with 0.15 μg/ml ethidium bromide. Gel images were acquired by using the Q-image digital imaging gel documentation system, and the band intensities were quantified by using IP Labs software. All experiments were done at least twice and a representative dataset is shown.

DSB Analysis

Genomic DNA was prepared as described (Sambrook and Russell, 2001). The restriction enzymes used for HO cutting, gene conversion and 5′–3′ resection analysis are StyI (New England Biolabs), EcoRI, HindIII, and SalI (Roche). The digested fragments were resolved on agarose gels (SeaKem ME agarose) and transferred to GeneScreen Plus hybridization membrane either by vacuum or capillary wet transfer. The DNA probes used for Southern blotting are prepared by Amersham DNA labeling beads ($-$dCTP) and purified by Amersham G-50 Micro Columns. Blot radioactivity was detected with a Molecular Dynamics Phosphor Imager and quantified with IP Labs software.

PFGE Analysis

Total chromosomal DNA agarose plugs were prepared as described (Schwartz and Cantor, 1984) and resolved on a 1% agarose gel by using Bio-Rad CHEF-DR III system at 6 V/cm for 24 hr with a switch time ramped from 60 to 120 s at 14°C.

Gamma Irradiation

Gamma irradiation was done by using a ^{137}Cs source with a radiation dose of 16 Gy/min (Mark I irradiator; J.L. Shepherd and Associates).

Acknowledgments

We thank Christophe Redon for providing the γ-H2AX antiserum and for his help during the gamma irradiation studies; Camilla Sjögren for communicating results prior to publication; Yixian Zhang, Orna Cohen-Fix, Margaret Hoang, Hong-Guo Yu, and Dongli Huang for constructive comments on the manuscript; Eileen Hogan, Cathy Mistrot, Ellen Cammon, and Patricia Cammon for technical support; and Terence Murphy, Judith Yanowitz, and members of our laboratories for advice and helpful discussions. D.K. is supported by grants from the Howard Hughes Medical Institutes and J.E.H is supported by National Institutes of Health grants GM20056 and GM61766 and by Department of Energy grant 01ER63229.

Received: July 27, 2004
Revised: October 6, 2004
Accepted: November 5, 2004
Published: December 21, 2004

References

Bernard, P., Maure, J.F., Partridge, J.F., Genier, S., Javerzat, J.P., and Allshire, R.C. (2001). Requirement of heterochromatin for cohesion at centromeres. Science *294*, 2539–2542.

Birkenbihl, R.P., and Subramani, S. (1992). Cloning and characterization of rad21 an essential gene of Schizosaccharomyces pombe involved in DNA double-strand-break repair. Nucleic Acids Res. *20*, 6605–6611.

Blat, Y., and Kleckner, N. (1999). Cohesins bind to preferential sites along yeast chromosome III, with differential regulation along arms versus the centric region. Cell *98*, 249–259.

Bradbury, J.M., and Jackson, S.P. (2003). The complex matter of DNA double-strand break detection. Biochem. Soc. Trans. *31*, 40–44.

Burma, S., Chen, B.P., Murphy, M., Kurimasa, A., and Chen, D.J. (2001). ATM phosphorylates histone H2AX in response to DNA double-strand breaks. J. Biol. Chem. *276*, 42462–42467.

Ciosk, R., Shirayama, M., Shevchenko, A., Tanaka, T., Toth, A., and Nasmyth, K. (2000). Cohesin's binding to chromosomes depends on a separate complex consisting of Scc2 and Scc4 proteins. Mol. Cell *5*, 243–254.

D'Amours, D., and Jackson, S.P. (2002). The Mre11 complex: at the crossroads of dna repair and checkpoint signalling. Nat. Rev. Mol. Cell Biol. *3*, 317–327.

Digweed, M., Reis, A., and Sperling, K. (1999). Nijmegen breakage syndrome: consequences of defective DNA double strand break repair. Bioessays *21*, 649–656.

Downs, J.A., Lowndes, N.F., and Jackson, S.P. (2000). A role for Saccharomyces cerevisiae histone H2A in DNA repair. Nature *408*, 1001–1004.

Frank-Vaillant, M., and Marcand, S. (2002). Transient stability of DNA ends allows nonhomologous end joining to precede homologous recombination. Mol. Cell *10*, 1189–1199.

Glynn, E.F., Megee, P.C., Yu, H., Mistrot, C., Unal, E., Koshland, D.E., DeRisi, J.D., and Gerton, J.L. (2004). Genome-Wide Mapping of the Cohesin Complex in the Yeast Saccharomyces cerevisiae. PLoS Biol *2*, 1325–1339.

Guacci, V., Koshland, D., and Strunnikov, A. (1997). A direct link between sister chromatid cohesion and chromosome condensation revealed through the analysis of MCD1 in S. cerevisiae. Cell *91*, 47–57.

Guthrie, C., and Fink, G.R. eds. (1991). Guide to Yeast Genetics and Molecular Biology (New York: Academic Press, Inc.).

Haber, J.E. (2002). Uses and abuses of HO endonuclease. Methods Enzymol. *350*, 141–164.

Heo, S.J., Tatebayashi, K., Kato, J., and Ikeda, H. (1998). The RHC21 gene of budding yeast, a homologue of the fission yeast rad21+ gene, is essential for chromosome segregation. Mol. Gen. Genet. *257*, 149–156.

Ivanov, E.L., Sugawara, N., White, C.I., Fabre, F., and Haber, J.E. (1994). Mutations in XRS2 and RAD50 delay but do not prevent mating-type switching in Saccharomyces cerevisiae. Mol. Cell. Biol. *14*, 3414–3425.

Jackson, S.P. (2002). Sensing and repairing DNA double-strand breaks. Carcinogenesis *23*, 687–696.

Jensen, R.E., and Herskowitz, I. (1984). Directionality and regulation of cassette substitution in yeast. Cold Spring Harb. Symp. Quant. Biol. *49*, 97–104.

Kadyk, L.C., and Hartwell, L.H. (1992). Sister chromatids are preferred over homologs as substrates for recombinational repair in Saccharomyces cerevisiae. Genetics *132*, 387–402.

Kim, J.S., Krasieva, T.B., LaMorte, V., Taylor, A.M., and Yokomori, K. (2002a). Specific recruitment of human cohesin to laser-induced DNA damage. J. Biol. Chem. *277*, 45149–45153.

Kim, S.T., Xu, B., and Kastan, M.B. (2002b). Involvement of the cohesin protein, Smc1, in Atm-dependent and independent responses to DNA damage. Genes Dev. *16*, 560–570.

Kitagawa, R., Bakkenist, C.J., McKinnon, P.J., and Kastan, M.B. (2004). Phosphorylation of SMC1 is a critical downstream event in the ATM-NBS1-BRCA1 pathway. Genes Dev. *18*, 1423–1438.

Koshland, D.E., and Guacci, V. (2000). Sister chromatid cohesion: the beginning of a long and beautiful relationship. Curr. Opin. Cell Biol. *12*, 297–301.

Laloraya, S., Guacci, V., and Koshland, D. (2000). Chromosomal addresses of the cohesin component Mcd1p. J. Cell Biol. *151*, 1047–1056.

Lee, J.H., and Paull, T.T. (2004). Direct activation of the ATM protein kinase by the Mre11/Rad50/Nbs1 complex. Science *304*, 93–96.

Lee, S.E., Moore, J.K., Holmes, A., Umezu, K., Kolodner, R.D., and Haber, J.E. (1998). Saccharomyces Ku70, mre11/rad50 and RPA proteins regulate adaptation to G2/M arrest after DNA damage. Cell *94*, 399–409.

Megee, P.C., Mistrot, C., Guacci, V., and Koshland, D. (1999). The centromeric sister chromatid cohesion site directs Mcd1p binding to adjacent sequences. Mol. Cell *4*, 445–450.

Michaelis, C., Ciosk, R., and Nasmyth, K. (1997). Cohesins: chromosomal proteins that prevent premature separation of sister chromatids. Cell *91*, 35–45.

Michelson, R.J., and Weinert, T. (2000). Closing the gaps among a web of DNA repair disorders. Bioessays *22*, 966–969.

Moore, J.K., and Haber, J.E. (1996). Capture of retrotransposon DNA at the sites of chromosomal double-strand breaks. Nature *383*, 644–646.

Nasmyth, K. (2002). Segregating sister genomes: the molecular biology of chromosome separation. Science *297*, 559–565.

Nickoloff, J.A., Chen, E.Y., and Heffron, F. (1986). A 24-base-pair DNA sequence from the MAT locus stimulates intergenic recombination in yeast. Proc. Natl. Acad. Sci. USA *83*, 7831–7835.

Nonaka, N., Kitajima, T., Yokobayashi, S., Xiao, G., Yamamoto, M., Grewal, S.I., and Watanabe, Y. (2002). Recruitment of cohesin to heterochromatic regions by Swi6/HP1 in fission yeast. Nat. Cell Biol. *4*, 89–93.

Paques, F., Leung, W.Y., and Haber, J.E. (1998). Expansions and contractions in a tandem repeat induced by double-strand break repair. Mol. Cell. Biol. *18*, 2045–2054.

Partridge, J.F., Scott, K.S., Bannister, A.J., Kouzarides, T., and Allshire, R.C. (2002). cis-acting DNA from fission yeast centromeres mediates histone H3 methylation and recruitment of silencing factors and cohesin to an ectopic site. Curr. Biol. *12*, 1652–1660.

Pellicioli, A., Lee, S.E., Lucca, C., Foiani, M., and Haber, J.E. (2001). Regulation of Saccharomyces Rad53 checkpoint kinase during adaptation from DNA damage-induced G2/M arrest. Mol. Cell *7*, 293–300.

Redon, C., Pilch, D.R., Rogakou, E.P., Orr, A.H., Lowndes, N.F., and Bonner, W.M. (2003). Yeast histone 2A serine 129 is essential for the efficient repair of checkpoint-blind DNA damage. EMBO Rep. *4*, 678–684.

Rogakou, E.P., Pilch, D.R., Orr, A.H., Ivanova, V.S., and Bonner, W.M. (1998). DNA double-stranded breaks induce histone H2AX phosphorylation on serine 139. J. Biol. Chem. *273*, 5858–5868.

Rogakou, E.P., Boon, C., Redon, C., and Bonner, W.M. (1999). Megabase chromatin domains involved in DNA double-strand breaks in vivo. J. Cell Biol. *146*, 905–916.

Rotman, G., and Shiloh, Y. (1998). ATM: from gene to function. Hum. Mol. Genet. *7*, 1555–1563.

Rouse, J., and Jackson, S.P. (2002). Interfaces between the detection, signaling, and repair of DNA damage. Science *297*, 547–551.

Sambrook, J., and Russell, D.W. (2001). Molecular Cloning: A Laboratory Manual, Third Edition (Cold Spring Harbor, NY: Cold Spring Harbor Laboratory Press).

Schwartz, D.C., and Cantor, C.R. (1984). Separation of yeast chromosome-sized DNAs by pulsed field gradient gel electrophoresis. Cell *37*, 67–75.

Shiloh, Y. (2001). ATM and ATR: networking cellular responses to DNA damage. Curr. Opin. Genet. Dev. *11*, 71–77.

Shiloh, Y. (2003). ATM and related protein kinases: safeguarding genome integrity. Nat. Rev. Cancer *3*, 155–168.

Shroff, R., Arbel-Eden, A., Pilch, D., Ira, G., Bonner, W.M., Petrini, J.H., Haber, J.E., and Lichten, M. (2004). Distribution and dynamics of chromatin modification induced by a defined DNA double-strand break. Curr. Biol. *14*, 1703–1711.

Sidorova, J.M., and Breeden, L.L. (2003). Rad53 checkpoint kinase phosphorylation site preference identified in the Swi6 protein of Saccharomyces cerevisiae. Mol. Cell. Biol. *23*, 3405–3416.

Sjögren, C., and Nasmyth, K. (2001). Sister chromatid cohesion is required for postreplicative double-strand break repair in Saccharomyces cerevisiae. Curr. Biol. *11*, 991–995.

Sonoda, E., Matsusaka, T., Morrison, C., Vagnarelli, P., Hoshi, O., Ushiki, T., Nojima, K., Fukagawa, T., Waizenegger, I.C., Peters, J.M., et al. (2001). Scc1/Rad21/Mcd1 is required for sister chromatid cohesion and kinetochore function in vertebrate cells. Dev. Cell *1*, 759–770.

Stiff, T., O'Driscoll, M., Rief, N., Iwabuchi, K., Lobrich, M., and Jeggo, P.A. (2004). ATM and DNA-PK function redundantly to phosphorylate H2AX after exposure to ionizing radiation. Cancer Res. *64*, 2390–2396.

Ström, L., Betts Lindroos, H., Shirahige, K., and Sjögren, C. (2004). Postreplicative recruitment of cohesin to double-strand breaks is required for DNA repair. Mol. Cell *16*, this issue, 1003–1015.

Tanaka, T., Cosma, M.P., Wirth, K., and Nasmyth, K. (1999). Identification of cohesin association sites at centromeres and along chromosome arms. Cell *98*, 847–858.

Uhlmann, F., and Nasmyth, K. (1998). Cohesion between sister chromatids must be established during DNA replication. Curr. Biol. *8*, 1095–1101.

Ward, I.M., and Chen, J. (2001). Histone H2AX is phosphorylated in an ATR-dependent manner in response to replicational stress. J. Biol. Chem. *276*, 47759–47762.

Yazdi, P.T., Wang, Y., Zhao, S., Patel, N., Lee, E.Y., and Qin, J. (2002). SMC1 is a downstream effector in the ATM/NBS1 branch of the human S-phase checkpoint. Genes Dev. *16*, 571–582.